Clinical Science (2018) **00** 1–14
https://doi.org/10.1042/CS20180944

PORTLAND PRESS

Research Article

Poldip2 deficiency protects against lung edema and vascular inflammation in a model of acute respiratory distress syndrome

Steven J. Forrester[1,*], Qian Xu[1,2,*], Daniel S. Kikuchi[1], Derick Okwan-Duodu[1], Ana Carolina Campos[1], Elizabeth A. Faidley[1], Guogang Zhang[2], Bernard Lassègue[1], Ruxana T. Sadikot[3,4], Kathy K. Griendling[1] and Marina S. Hernandes[1]

[1]Division of Cardiology, Department of Medicine, Emory University, Atlanta, GA 30322, U.S.A.; [2]Department of Cardiovascular Medicine, Xiangya Hospital, Central South University, Changsha 410008, China ; [3]Department of Veterans Affairs, Atlanta VAMC; [4]Division of Pulmonary and Critical Care Medicine, Department of Medicine, Emory University, Atlanta, GA 30322, U.S.A.

Correspondence: Marina Sorrentino Hernandes (mshern2@emory.edu)

Acute respiratory distress syndrome (ARDS) in a deadly disease that can be brought on by endotoxins such as lipopolysaccharide (LPS). ARDS is characterized by vascular permeability, a severe inflammatory response, lung leukocyte infiltration, and resultant lung edema. Polymerase δ-interacting protein 2 (Poldip2) is a novel regulator of blood–brain barrier permeability; however, its role in regulating lung permeability and vascular inflammation is unknown. Here, the role of Poldip2 in regulating vascular permeability and inflammation in a mouse model of ARDS was assessed. Heterozygous deletion of Poldip2 was found to reduce LPS-induced mortality within 20 h, lung inflammatory signaling, and leukocyte infiltration. Moreover, reduced Poldip2-suppressed LP-induced vascular cell adhesion molecule (VCAM)-1 induction, leukocyte recruitment, and mitochondrial reactive oxygen species (ROS) production *in vitro*. These data indicate that Poldip2 is an important regulator of the debilitating consequences of ARDS, potentially through the regulation of mitochondrial ROS-induced inflammatory signaling. Consequently, inhibition of Poldip2 may be a viable option for therapeutic discovery moving forward.

Introduction

Acute respiratory distress syndrome (ARDS) is an inflammatory lung condition that affects approximately 200000 patients annually in the United States, resulting in nearly 74500 deaths [1]. With a current severity-dependent mortality rate ranging from 35 to 46%, ARDS accounts for 10% of intensive care unit admissions according to a recent prospective cohort study carried out in 50 different countries [2]. ARDS can be caused by a variety of pulmonary (e.g., pneumonia, aspiration, toxic inhalation, lung contusion) or non-pulmonary (e.g., sepsis, trauma, pancreatitis) events, and therapeutic strategies are limited to the treatment of the underlying disease [3], accompanied by mechanical ventilation for ARDS management [4]. Severe sepsis is considered the most common cause of ARDS, accounting for around 79% of cases [1]. ARDS has been shown to induce pulmonary vascular permeability and inflammation, which results in leukocyte infiltration into the lung and loss of aerated lung tissue. Such events are major contributors to hypoxemia, which is a critical event that defines ARDS [5]. Because of the complex nature of the disease, blocking individual pro-inflammatory cytokines with antibodies is ineffective; a better approach is to define the contribution of proximal signaling pathways that amplify the inflammatory response and to develop targeted therapies to specifically block them in order to limit injury and inflammation for this devastating disease.

[*] These authors contributed equally to this work.

Received: 26 October 2018
Revised: 19 December 2018
Accepted: 07 January 2019

Accepted Manuscript Online: 08 January 2019
Version of Record published: 00 xx 00

Clinical Science (2018) **00** 1–14
https://doi.org/10.1042/CS20180944

Multiple cell types contribute to the pathogenesis of lung injury, including structural and immune cells. The intense inflammatory response in the pulmonary endothelium is characterized by endothelial cell (EC) activation [6], increased cytokine and chemokine release [7], destabilization of adherens junctions and interendothelial gap formation [8,9]. In addition, alterations in cell–cell adhesion is a key step in ARDS development [10]. Increased pulmonary EC-leukocyte interaction facilitates leukocyte transmigration from the capillaries into the lung parenchyma, contributing to the inflammatory response as well as to pulmonary edema formation [10]. Transmigration of leukocytes is mediated by their firm adhesion to ECs through the interaction of β2 integrins on circulating leukocytes to adhesion molecules such as vascular cell adhesion molecule (VCAM)-1 on activated ECs [11].

VCAM-1 expression on ECs is induced by several mediators, including cytokines, high glucose, and stimulation of endothelial toll-like receptors [12]. Importantly, it is well-recognized that VCAM-1 expression is regulated by reactive oxygen species (ROS) [12]. In response to inflammatory agonists, NADPH oxidase-derived ROS promote nuclear factor κB (NF-κB) and AP-1-dependent gene transcription of adhesion molecules, including VCAM-1. In addition, there is an increasing appreciation for the role of mitochondrial-derived ROS (mitoROS) in the regulation of NF-κB-dependent gene induction [13]. However, less is known about the mechanisms that regulate inflammation-induced mitoROS production compared with cytoplasmic ROS.

Polymerase δ-interacting protein 2 (Poldip2) is a multifunctional protein first described as a DNA polymerase-δ and proliferating cell nuclear antigen binding partner [14]. In addition to its role in DNA replication and damage repair, there is evidence that Poldip2 plays a pathophysiological role in cancer development. Poldip2 gene mutations were found in soft tissue sarcoma [15] and Poldip2 gene expression was found strongly correlated with breast cancer tumors [16].Our group has recently reported that Poldip2 mediates the breakdown of the blood–brain barrier (BBB) in response to cerebral ischemia by increasing cytokine production and MMP activation [17]. Moreover, heterozygous deletion of Poldip2 reduces ROS production *in vivo*, leading to increases in extracellular matrix deposition and vascular stiffness [18]. Based on the very clear phenotype of impaired ROS production and reduced BBB permeability induced by cerebral ischemia in mice heterozygous for Poldip2, we hypothesized that Poldip2 may play a universal role controlling EC activation and leukocyte infiltration into the lung tissue during sepsis-induced ARDS. In the present study, we reveal a crucial role for Poldip2 in regulating lipopolysaccharide (LPS)-induced leukocyte extravasation into the lung tissue. Our data suggest that Poldip2$^{+/-}$ mice exhibit reduced mortality, as well as reduced cytokine, chemokine, and VCAM-1 induction, following LPS-induced ARDS. We further show that Poldip2 reduction in cultured human primary pulmonary microvascular endothelial cells (HPMECs) attenuates VCAM-1 expression and monocyte adhesion through attenuation of LPS-induced mitoROS production. Our findings uncover a previously unknown role of Poldip2 in leukocyte recruitment, suggesting novel approaches to improve pulmonary EC barrier function in ARDS.

Materials and methods

Animals

Adult male and female (20–30 g) mice with C57BL/6J background mice were used in the present study. Poldip2 gene trap mice on a C57BL/6 background were produced by the Texas A&M Institute for Genomic Medicine [18]. Mice were genotyped using a standard three-primer PCR method. As noted previously [18], Poldip2 homozygous deletion is embryonically lethal, and so Podip2 heterozygote mice (Poldip2$^{+/-}$) were used in the present study. All animal experiments were conducted with the approval of the Institutional Animal Care and Use Committee at Emory University (protocol reference number: 3000399). Ethical approval was received before conducting the study. For reported data, researchers performing analyses were blinded to genotype and experimental grouping of mice.

LPS-induced ARDS

Poldip2$^{+/+}$ and Poldip2$^{+/-}$ mice were randomly divided into PBS and LPS groups. Animals received an intraperitoneal (i.p.) injection of LPS (18 mg/kg) from *Escherichia coli* 0111:B4 (InvivoGen, tlrl-eblps) diluted in PBS. An equal volume of PBS was given to mice in the control group. For survival analysis, mice were injected and mortality-monitored every hour. Initial findings showed a majority of Poldip2$^{+/+}$ mice treated with LPS did not survive past 20 h, whereas all other groups did. Due to the high mortality in the Poldip2$^{+/+}$ LPS group, 20 h was chosen as the survival analysis cutoff time. For bronchoalveolar lavage (BAL) fluid and lung tissue analyses, all mice were sacrificed 6 or 18 h after LPS treatment. Systemic blood samples (10 μl) were taken after the LPS administration and assessed for white blood cell count using a hemocytometer.

BAL collection

Mouse tracheas were exposed through a small skin incision on the anterior neck and cannulated using a 21-gauge lavage needle. For assessment of cytokine and chemokines, 1.2 ml of PBS was instilled in the tracheal lavage needle and retrieved. Return volume was centrifuged (300 ***g***, 10 min), and the supernatant was stored at −80°C for assessment of cytokine and chemokines levels. For determination of total cell counts in BAL, three lavages with 1 ml each of PBS were pooled from each animal. The BAL fluid was then spun at 300 ***g*** for 10 min at 4°C. Pellets were resuspended for either total leukocyte counts or for flow cytometric analyses. For leukocyte counts, the cell pellet was suspended in serum-free RPMI 1640 culture medium and total cell counts were determined using a Countess II FL Automated Cell Counter (Thermo Fisher, U.S.A.).

Chemokine and cytokine ELISAs

Monocyte chemotactic protein-1 (MCP-1) interleukin (IL)-1β, IL-6, tumor necrosis factor-α (TNF-α), and chemokine (C-X-C motif) ligand 1 (CXCL-1) levels in BAL fluids were measured using specific ELISA kits according to the manufacturer's instructions (R&D Systems).

Flow cytometry

Cells were blocked with anti-mouse CD16/32 (Biolegend) for 5 minutes followed by incubation with anti-mouse antibodies for 30 min on ice. Cells were then washed with FACs buffer (Biolegend) and subjected to flow cytometry on a Cytoflex flow cytometer (Beckman). The following antibodies (Biolegend) were used: APC-CD45, FITC-CD31, BV405-Ly6G, and PerCy7-CD11b. Data were analyzed with the FLowJo software package (Tree Star). Leukocytes were identified as $CD45^{+}CD31^{-}$, neutrophils as $Ly6G^{+}CD11b^{+}$ cells, and monocytes as $CD11b^{high}Ly6G^{low}$. Isotype-matched antibodies were used as negative controls. For complete blood counts (CBC), white blood cells were counted by a Hemavet 1500 blood analyzer (CDC Technologies, Oxford, CT).

RNA extraction and RT-qPCR

Total RNA was purified with the RNeasy Plus kit (Qiagen). Reverse transcription was performed using Superscript II reverse transcriptase (Invitrogen) with random primers and cDNA was purified with the QIAquick kit (Qiagen). The cDNA was amplified with primers against ribosomal protein L13A (RPL) (5′-ATGACAAGAAAAAGCGGATG-3′, 5′-CTTTTCTGCCTGTTTCCGTA-3′, - 58°C), TNF-α (5′-CTATGTCTCAGCCTCTTCTC-3′, 5′-CATTTGGGAACTTCTCATCC-3′, 52°C), MCP-1 (5′-AGCACCAGCCAACTCTCACT -3′, 5′-TCTGGACCCATTCCTTCTTG -3′, 63°C), intercellular adhesion molecule 1 (ICAM-1) (5′- CAAGGAGGACCTCAGCCTGG-3′, 5′- GGTGAGGTCCTTGCCTACTT-3′, 65°C) and VCAM-1 (5′- CCTTAATTGCTATGAGGATGG-3′, 5′- CCATTGAGGGGACTGTCTG-3′, 60°C) using Platinum Taq DNA polymerase (Invitrogen) and SYBR green I (Invitrogen). Reactions were carried out in glass capillaries using a LightCycler 1.2 (Roche Applied Science) real time thermocycler. Data analysis was performed using the mak3 module of the qpcR software library (version 1.4-0) [19,20] in the R-environment [21]. Because expression of RPL mRNA was not affected by the treatment, it was used to correct the measurements of other gene products and thereby reduced variability between samples. Final quantification results were expressed in arbitrary units.

Cell culture

HPMECs were purchased from Promocell and were cultured in EC growth medium (MV2 kit, C-22121, Promocell) supplemented with 5% FBS, 5 ng/ml human recombinant epidermal growth factor, 10 ng/ml human recombinant basic fibroblast growth factor, 20 ng/ml insulin-like growth factor, 0.5 ng/ml human recombinant vascular endothelial growth factor 165, 1 μg/ml ascorbic acid, and 0.2 μg/ml hydrocortisone. Media were changed every 2 days until cells reached confluence. All experiments were conducted between passages 4 and 7. In each experiment, cultures exposed to LPS (100 ng/ml) were compared with PBS control conditions. THP-1 monocytes were purchased from ATCC and cultured in RPMI-1640 (ATCC, #30-2001) supplemented with 10% FBS (Benchmark, #100-106) and penicillin and streptomycin (ThermoFisher, #15140).

Small interfering RNA

For Poldip2 silencing studies, confluent HPMECs were transfected with human small interfering RNA against Poldip2 (siPoldip2; sense: 5′- CGUGAGGUUUGAUCAGUAAdTdT- -3′, antisense: 5′-UUACUGAUCAAACCUCACGdTdG-3′; Qiagen) or the Allstars control small interfering RNA (siRNA) (siControl; sense: 5′-GGGUAUCGACGAUUACAAAUU-3′, antisense: 5′-UUUGUAAUCGUCGAUACCCUG-3′; Qiagen).

Clinical Science (2018) **00** 1–14
https://doi.org/10.1042/CS20180944

Cells were washed with HBSS, and incubated with siRNA + oligofectamine complexes in 2% serum OPTIMEM for 5 h. After transfection, OPTIMEM was then changed to MV2 media for an additional 48 h until LPS treatment was performed. Gene silencing was confirmed using immunoblotting. Cells were transfected with a final siRNA concentration of 100 nmol/l.

Western blotting

Whole cell lysate was prepared from cultured HPMECs using 1× sample buffer (0.5 M Tris-HCL pH 6.8, 10% (w/v) SDS, 6% β-mercaptoethanol, 10% glycerol, 100 mM dithiothreitol, 0.1% bromophenol blue). Homogenates were centrifuged at 12000 rpm at 4°C for 2 min and then sonicated for 10 s (30 amplitude). Homogenates were then spun down again and boiled for 3 min before storing at −20°C until gel loading. Following separation by SDS–PAGE, proteins were transferred to a nitrocellulose membrane and assessed by Western blotting with primary antibodies against Poldip2 (ab181841; Abcam), VCAM-1 (ab134047; Abcam), β-actin (A5441; Sigma), or GAPDH (mab374; Millipore). Blots were incubated with horseradish peroxidase (HRP)-conjugated secondary antibodies depending on the species of the primary antibody (anti-mouse [NA931; GE] and anti-rabbit [70745; Cell Signaling]) and assessed using enhanced chemiluminescence (ECL, GE). HRP-induced luminescence was detected with Amersham Hyperfilm ECL (GE). Detected bands were scanned and densitometry was performed using ImageJ.

THP-1 adhesion assay

For adhesion assays, THP-1 monocytes were spun down at 1500 rpm, 5 min, 20°C and resuspended in serum-free Dulbecco's Modified Eagle's Medium (DMEM, Sigma, D5671) supplemented with 0.2% BSA (Sigma, #3117332001), 2 mM L-glutamine (ThermoFisher, #25030), penicillin, and streptomycin. THP-1 cells were then incubated with 5 μg/ml Hoechst 33342 (ThermoFisher, #62249) for 10 min at 37°C to label nuclei. THP-1 cells were then spun down, washed with DMEM, re-spun and then re-suspended in fresh DMEM with 0.2% BSA (7×10^4 cells per ml). For LPS experiments, confluent HPMECs transfected with control or Poldip2 siRNA were stimulated with PBS or LPS (100 ng/ml) for 6 h prior to the adhesion assay. After 6 h, HPMECs were washed once with 0.2% BSA DMEM followed by addition of THP-1 cells (3.5×10^4 cells per well, 24-well plate). THP-1 and HPMECs were incubated together for 30 min at 37°C. Cells were then washed twice with warm PBS followed by fixation in 3.7% paraformaldehyde (Electron Microscopy Science, #15714-S) for 10 min at room temperature. Fixed cells were washed once in PBS and immediately imaged using a 10× objective lens. Images were acquired on an Olympus IX71 Inverted fluorescent microscope with a DAPI fluorescent filter. Three representative pictures were acquired per sample. Images were imported using ImageJ (NIH). Background was subtracted from images and an image threshold was generated. Stained THP-1 nuclei were counted using the analyze particles function to evaluate adhesion to HPMECs.

Mitochondrial ROS assay

To measure mitochondrial ROS production, we utilized the mitoTimer reporter construct [22]. Briefly, mitoTimer encodes the mitochondria-targeted DsRed1-E5 fluorescent reporter that fluoresces green when expressed. Upon interaction with ROS, the probe shifts irreversibly to red. Relative ROS production is determined by measuring the red to green ratio. An adenovirus encoding the mitoTimer vector (Addgene, #52659) was generated using the ViraPowery™ Adenoviral Expression System (Invitrogen) according to manufacturer's instructions. For mitoROS measurements, HPMECs were grown on glass coverslips and transfected with control or Poldip2 siRNA 24 h prior to adenovirus transduction. HPMECs were transduced with the mitoTimer adenovirus (25 MOI) in normal media for 24 h. After 24 h, HPMECs were washed and fresh growth media was added. Eight hours later, HPMECs were stimulated with either PBS or LPS (100 ng/ml) and were incubated overnight. The next morning, HPMECs were washed once with PBS and fixed in HBSS containing 3.7% paraformaldehyde on ice for 10 min. HPMECs were washed twice with PBS and permeabilized in 0.2% Triton X-100 in PBS for 5 min. HPMECs were then washed twice and then mounted with Prolong Diamond with DAPI Antifade Solution (ThermoFisher, #P36962). Images were acquired on a Zeiss LSM 800 confocal laser scanning microscope using a 63× oil immersion objective (1.4 numerical aperture) green (488 nM) and red (561 nM) laser channels using the supplied Zen blue software application. A minimum of 25 cells per condition were analyzed for each independent experiment, and a total of four independent experiments were conducted. Red to green ratio was calculated after background subtraction by dividing the red fluorescence intensity value by the green fluorescence intensity value.

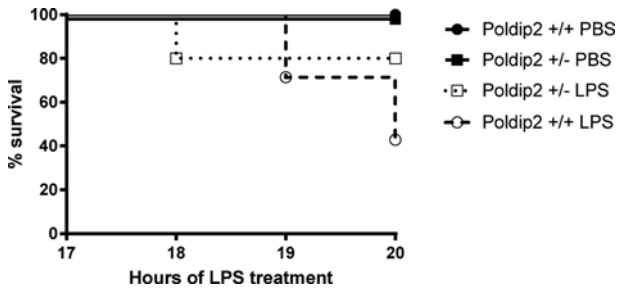

Figure 1. Heterozygous deletion of Poldip2 improves survival

Survival rates in Poldip2$^{+/+}$ and Poldip2$^{+/-}$ mice after LPS treatment. Male and female Poldip2$^{+/+}$ and Poldip2$^{+/-}$ mice (seven to eight mice per group) were treated with PBS or LPS. Kaplan–Meier survival curves indicate a significant increase in survival of Poldip2$^{+/-}$ mice compared with Poldip2$^{+/+}$ animals 20 h after LPS injection (P=0.03).

MitoTEMPO

For MitoTEMPO experiments, HPMECs were pre-treated with 1 mM mitoTempo (Sigma, SML0737) before treatment with PBS or LPS (100 ng/ml) for 6 h.

Statistical analysis

Data are expressed as mean ± S.E.M. Statistical analyses were performed using two-way ANOVA with a Tukey's multiple comparison test. $P<0.05$ was considered statistically significant. Survival curve (Kaplan–Meier curve) was analyzed using the log-rank test.

Results

Heterozygous deletion of Poldip2 improves survival

To test the hypothesis that reduced Poldip2 decreases LPS-induced mortality we monitored survival during sepsis. We observed a significantly higher survival in Poldip2$^{+/-}$ mice compared with Poldip2$^{+/+}$ mice at 20 h following LPS treatment. While 80% of the Poldip2$^{+/-}$ mice survived 20 h after LPS injection, the survival percentage among the Poldip2$^{+/+}$ group was approximately 43% using Kaplan–Meier survival analysis (Figure 1).

Poldip2 regulates the recruitment of immune cells into the lung following LPS-induced ARDS

Given the reduced mortality of Poldip2$^{+/-}$ mice and the previously described effect of Poldip2 on BBB permeability [17], we sought to investigate the contribution of Poldip2 in leukocyte recruitment into the lungs after LPS-induced ARDS. Leukocyte recruitment to the lungs was determined in BAL fluids recovered 18 h after LPS treatment. LPS induced a marked increase in leukocyte infiltration into the lungs of Poldip2$^{+/+}$ mice, which was not observed in Poldip2$^{+/-}$ animals (Figure 2A). Flow cytometry was performed in leukocytes isolated from BAL fluids to further characterize the invading cell populations 6 and 18 h following LPS-induced ARDS. As indicated in Figure 2B, the infiltration of CD11b^{high}Ly6G^{low} inflammatory monocytes was significantly reduced at 6 h in Poldip2$^{+/-}$ mice treated with LPS when compared with Poldip2$^{+/+}$ mice. Likewise, Poldip2$^{+/-}$ mice treated with LPS exhibited reduced Ly6G^{+}CD11b^{+} neutrophil infiltration into the lungs at 6 and 18 h when compared with Poldip2$^{+/+}$ mice treated with LPS (Figure 2C). Systemic leukocyte counts were similar between Poldip2$^{+/+}$ and Poldip2$^{+/-}$ mice at 6 and 18 h following LPS (Supplementary Figure S1).

Poldip2 reduction abrogates cytokine and chemokine induction *in vivo*

ARDS-induced leukocyte infiltration is associated with increased production of several cytokines and chemokines [23,24]. To determine whether Poldip2 regulates cytokine and chemokine induction, we first examined their mRNA and expression levels. Six hours post LPS injection, lung TNF-α, MCP-1, IL-1β, and IL-6 mRNA levels were measured. As shown in Figure 3A, TNF-α, MCP-1, and IL-1β mRNA levels were dramatically increased 6 h after LPS in the lungs of Poldip2$^{+/+}$ mice, but not or to a lesser degree in Poldip2$^{+/-}$ animals (Figure 3A). In contrast, LPS-induced IL-6 mRNA expression was not affected by Poldip2 reduction. Additionally, TNF-α, MCP-1, IL-1β, IL-6, and CXCL-1 protein levels were evaluated in BAL fluids of Poldip2$^{+/+}$ and Poldip2$^{+/-}$ mice using ELISAs. Corroborating the mRNA

Clinical Science (2018) **00** 1–14
https://doi.org/10.1042/CS20180944

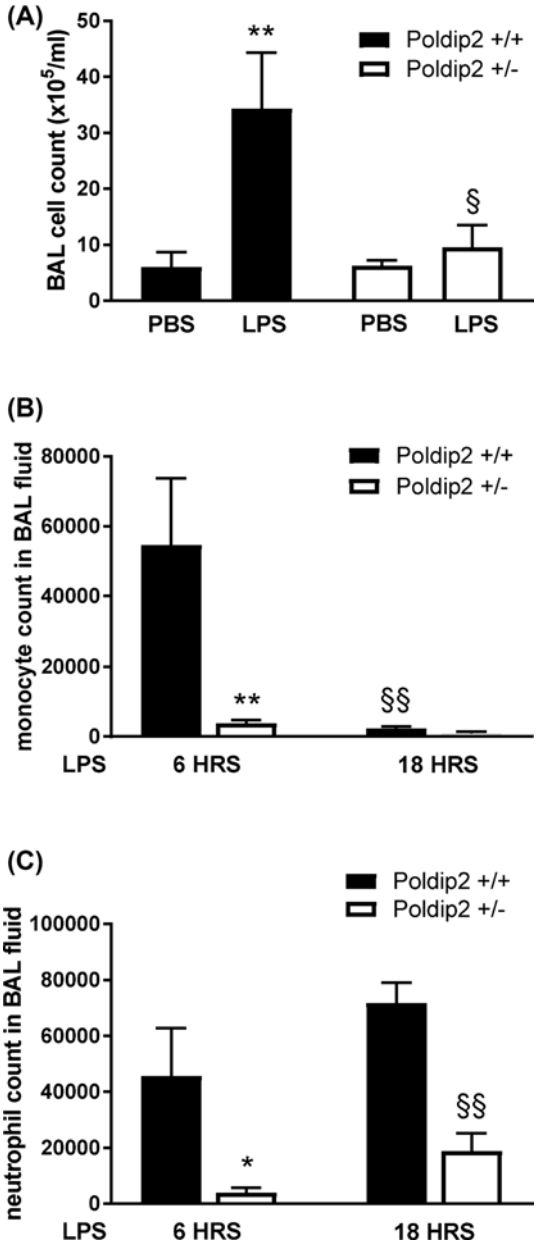

Figure 2. Poldip2 regulates the recruitment of leukocytes following LPS-induced ARDS

(**A**) Comparison between the total number of cells in the BAL fluid of Poldip2$^{+/+}$ and Poldip2$^{+/-}$ mice 18 h after PBS or LPS injection. The total number of leukocytes was determined using a hemocytometer. The bar graph represents means ± S.E.M. of four to five mice per group. Two-way ANOVA $^{**}P<0.01$ vs Poldip2$^{+/+}$ PBS $^{§}P<0.05$ vs Poldip2$^{+/+}$ LPS. (**B**) Analysis of specific CD11b^{high}Ly6G^{low} positive monocytes in the BAL fluid of Poldip2$^{+/+}$ and Poldip2$^{+/-}$ mice 6 and 18 h after LPS injection was performed by flow cytometry. The bar graph represents means ± S.E.M. of five to six mice per group. Two-way ANOVA $^{**}P<0.01$ vs Poldip2$^{+/+}$ 6 h LPS and $^{§§}P<0.01$ vs Poldip2$^{+/+}$ 6 h LPS. (**C**) Analysis of Ly6G^{+}CD11b^{+} neutrophils in the BAL fluid of Poldip2$^{+/+}$ and Poldip2$^{+/-}$ mice 6 and 18 h after LPS injection was performed by flow cytometry. The bar graph represents means ± S.E.M. of five to six mice per group. Two-way ANOVA $^{*}P<0.05$ vs Poldip2$^{+/+}$ LPS 6 h and $^{§§}P<0.01$ vs Poldip2$^{+/+}$ LPS 18 h.

expression data, TNF-α and MCP-1 protein levels were increased in the BAL fluid of Poldip2$^{+/+}$ mice after LPS but less so in Poldip2$^{+/-}$ mice (Figure 3B). Similar results were found for CXCL-1 protein levels (Figure 3B). IL-6 and IL-1β protein levels were not significantly increased in the BAL fluid of either Poldip2$^{+/+}$ or Poldip2$^{+/-}$ mice after LPS (Figure 3B).

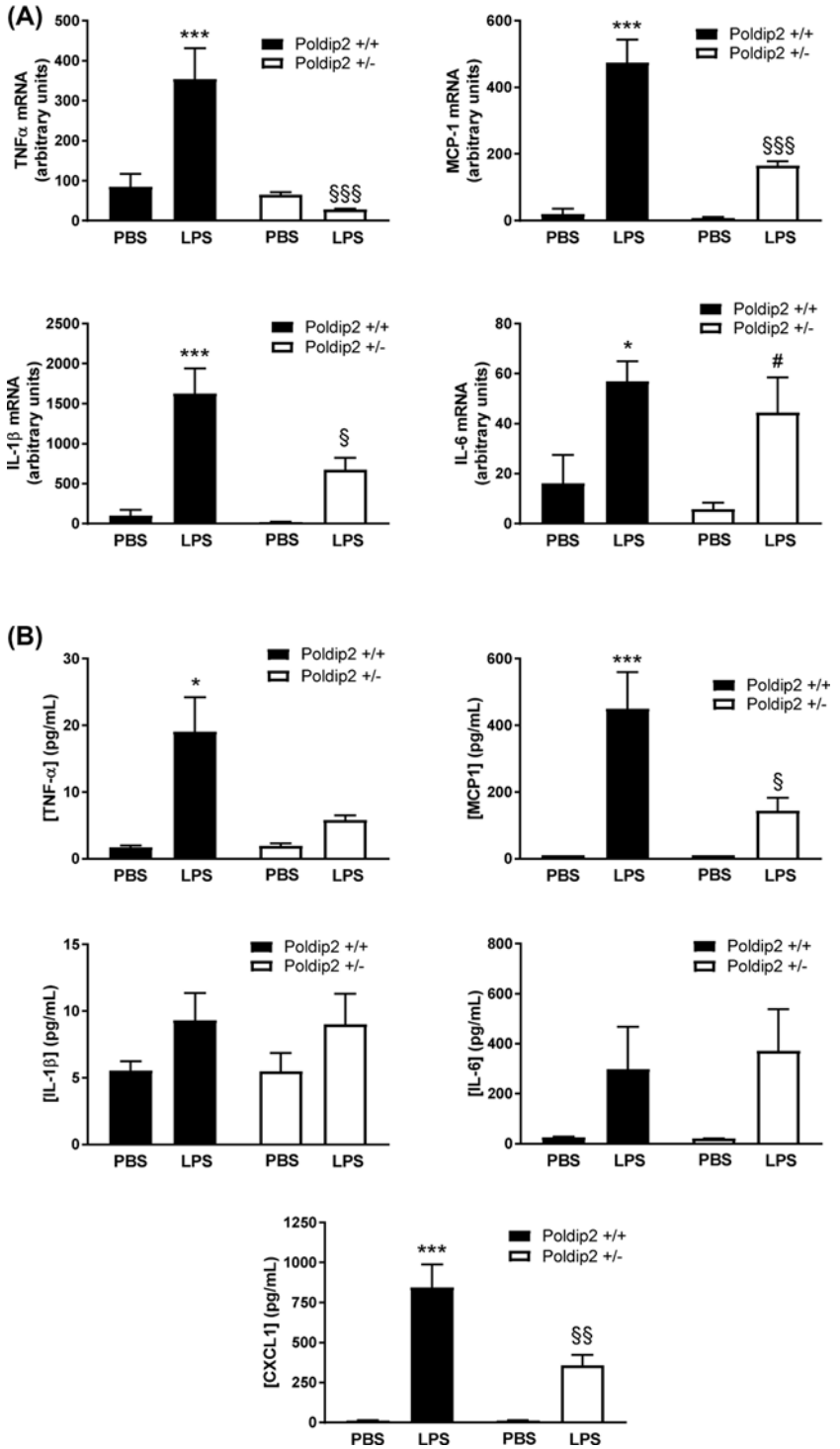

Figure 3. Poldip2 reduction abrogates cytokine and chemokine induction *in vivo*

Cytokine and chemokine mRNAs and protein were measured in the lung tissue and BAL fluid, 6 h after PBS or LPS in Poldip2$^{+/+}$ and $^{+/-}$ mice. (**A**) TNF-α, MCP-1 IL-1β, and IL-6 mRNAs were measured in the lung tissue by quantitative RT-PCR. Bar graphs represent means ± S.E.M. from five to nine mice per group. Two-way ANOVA $^{***}P<0.001$ vs Poldip2$^{+/+}$ PBS mice, $^{*}P<0.05$ vs Poldip2$^{+/+}$ PBS mice, $^{§§§}P<0.001$ vs Poldip2$^{+/+}$ LPS mice, $^{§}P<0.05$ vs Poldip2$^{+/+}$ LPS mice, and $^{\#}P<0.05$ vs Poldip2$^{+/-}$ PBS mice. (**B**) TNF-α, MCP-1, IL-1β, IL-6, and CXCL-1, proteins were measured by ELISA. Bar graphs represent means ± S.E.M. from four to six mice per group. Two-way ANOVA $^{*}P<0.05$ vs Poldip2$^{+/+}$ PBS mice, $^{***}P<0.001$ vs Poldip2$^{+/+}$ PBS mice, $^{§§}P<0.01$ vs Poldip2$^{+/+}$ LPS mice, and $^{§}P<0.05$ vs Poldip2$^{+/+}$ LPS mice.

Clinical Science (2018) **00** 1–14
https://doi.org/10.1042/CS20180944

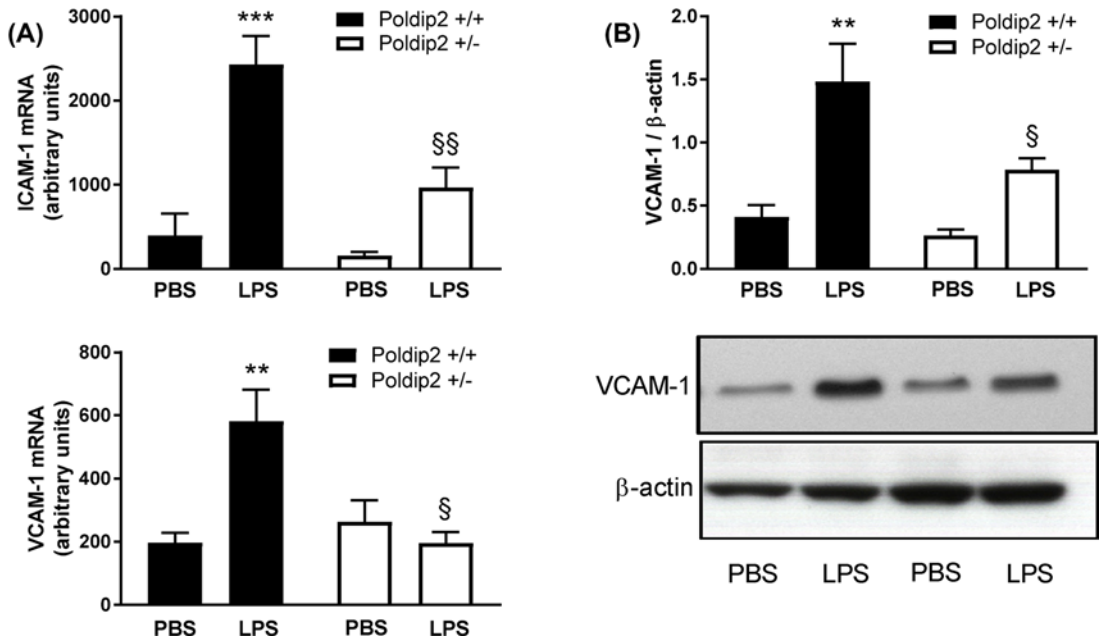

Figure 4. Heterozygous deletion of Poldip2 reduces the induction of leukocyte adhesion molecules *in vivo*

VCAM-1 and ICAM-1 mRNAs and proteins were measured in the lung tissue, 6 h after PBS or LPS in Poldip2$^{+/+}$ and $^{+/-}$ mice. (**A**) VCAM-1 and ICAM-1 mRNAs were measured in the lung tissue by quantitative RT-PCR. Bar graphs represent means ± S.E.M. from six to eight mice per group. Two-way ANOVA $^{***}P<0.001$ vs Poldip2$^{+/+}$ PBS mice, $^{**}P<0.01$ vs Poldip2$^{+/+}$ PBS mice, $^{§§}P<0.01$ vs Poldip2$^{+/+}$ LPS mice and $^{§}P<0.05$ vs Poldip2$^{+/+}$ LPS mice. (**B**) Mouse lungs were harvested and VCAM-1 was measured by Western blotting and densitometry. Representative blots are shown. The bar graph represents means ± S.E.M. of four to six independent experiments normalized to β-actin. $^{**}P<0.01$ vs Poldip2$^{+/+}$ PBS mice and $^{§}P<0.05$ vs Poldip2$^{+/+}$ LPS mice.

Heterozygous deletion of Poldip2 reduces leukocyte adhesion molecule induction *in vivo*

The first step in leukocyte infiltration involves adherence of leukocytes to the endothelium. The expression of VCAM-1 on the endothelium is a common occurrence in inflammatory diseases, including ARDS [25]. To determine the effect of heterozygous deletion of Poldip2 on expression of leukocyte adhesion molecules, Poldip2$^{+/+}$ and Poldip2$^{+/-}$ lung tissues were harvested 6 h after LPS injection and ICAM-1 and VCAM-1 mRNA levels were measured. Both ICAM-1 and VCAM-1 mRNA were significantly elevated by LPS in Poldip2$^{+/+}$ compared with PBS injected mice, and abrogated in Poldip2$^{+/-}$ mice (Figure 4A). We further analyzed VCAM-1 protein expression using Western blotting. As shown in Figure 4B, VCAM-1 protein expression was increased in the lung tissue of Poldip2$^{+/+}$ mice following LPS-induced ARDS; however, Poldip2$^{+/-}$ mice exhibited an attenuation of LPS-induced VCAM-1 expression compared with Poldip2$^{+/+}$ LPS mice (Figure 4B).

Poldip2 mediates leukocyte adhesion to ECs *in vitro*

To determine the role of Poldip2 in the regulation of VCAM-1 induction in ECs, we moved to an *in vitro* system. HPMECs were transfected with siPoldip2 or siControl and treated with LPS (100 ng/ml) for 6 h before assessing VCAM-1 protein levels. As expected from the *in vivo* data, siRNA against Poldip2 significantly inhibited LPS-induced VCAM-1 up-regulation (Figure 5A). Poldip2 depletion was confirmed by Western blotting (Figure 5A). The physiological consequence of this reduction in VCAM-1 was assessed by measuring THP-1 monocyte adherence. HPMECs were transfected with siPoldip2, stimulated with LPS for 6 h and then incubated with THP-1 monocytes. Similar to the effect of Poldip2 depletion on LPS-induced VCAM-1 expression, depletion of Poldip2 in HPMECs attenuated LPS-induced THP-1 adherence (Figure 5B), which suggests that endothelial Poldip2 may play a role in regulating leukocyte adherence during inflammation.

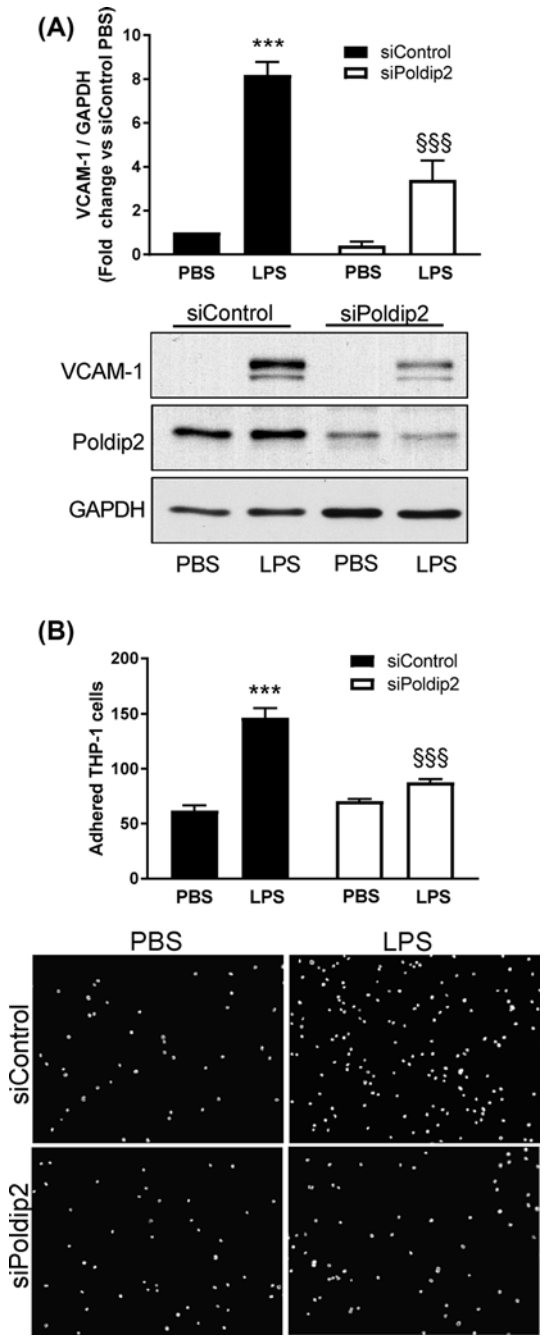

Figure 5. Poldip2 mediates VCAM-1 induction and THP-1 monocyte adhesion to HPMECs

Confluent HPMECs were transfected with siControl or siPoldip2 before exposure to PBS or LPS (100 ng/ml) for 6 h. (**A**) VCAM-1 protein expression was measured by Western blotting and densitometry. Down-regulation of Poldip2 after siRNA transfection was verified by Western blotting. Bars represent means ± S.E.M. of four independent experiments normalized to GAPDH. Results are presented as fold change with respect to siControl + PBS. Two-way ANOVA $^{***}P<0.001$ vs siControl PBS, $^{§§§}P<0.001$ vs siControl LPS. (**B**) Adhesion of THP-1 monocytes to HPMECs was determined by light microscopy. Bars represent means ± S.E.M. of four independent experiments. Two-way ANOVA $^{***}P<0.001$ vs siControl PBS and $^{§§§}P<0.001$ vs siControl LPS.

Clinical Science (2018) **00** 1–14
https://doi.org/10.1042/CS20180944

Silencing Poldip2 prevents LPS-induced mitoROS production

Due to the effects of Poldip2 on mitochondrial function and morphology [26,27], as well as overall cellular ROS production [18,28], we hypothesized that Poldip2 depletion in HPMECs would affect mitochondrial ROS production. To measure mitochondrial ROS production, siControl and siPoldip2-transfected cells were transduced with an adenovirus encoding the mitochondrial redox reporter mitoTimer [22]. In response to LPS, siControl HPMECs exhibited an increased red to green ratio, suggesting increased mitROS production in these cells. However, siPoldip2-transfected cells were largely protected from this response (Figure 6A), indicating silencing of Poldip2 may be protective against LPS-induced mitoROS production. We next sought to test the contribution of mitoROS to LPS-induced VCAM-1 induction in HPMECs. Prior to LPS stimulation, HPMECs were pre-treated with either H_2O or the mitoROS scavenger MitoTEMPO [29]. Unlike H_2O-treated conditions, which displayed marked VCAM-1 expression in response to LPS, VCAM-1 induction in HPMECs pre-treated with MitoTEMPO was attenuated (Figure 6B), indicating that mitoROS play a role in VCAM-1 up-regulation and may explain how Poldip2 influences inflammatory signaling.

Discussion

In the present study, we uncovered a novel role for Poldip2 in LPS-induced ARDS. Notably, heterozygous deletion of Poldip2 was observed to enhance survival and attenuate cytokine and chemokine induction and immune cell recruitment into the lungs of LPS-challenged mice. Moreover, our *in vitro* investigation indicated that Poldip2 promotes EC VCAM-1 induction and resultant leukocyte adhesion, potentially through its ability to modulate mitoROS production.

LPS is a major component of the bacterial cell outer membrane and has been widely used to induce ARDS in murine models [30]. Previous studies have demonstrated that LPS-challenged mice present typical pathological characteristics of ARDS, including increased pro-inflammatory cytokine induction, increased vascular permeability as well as alveolar fluid accumulation [31]. Leukocyte recruitment and migration through ECs appears to be a key initiator of the pathology associated with LPS-induced ARDS. Leukocyte activation and initial attachment and rolling on ECs is induced by the local secretion of inflammatory cytokines [32]. In mice, LPS has been shown to induce the production of several pro-inflammatory cytokines, including TNFα, IFNγ, IL-1β, IL-5, IL-6, IL-10, IL-12, MCP-1, MCP-5, and RANTES [33]. Consistent with those previous studies, we found that LPS induced the expression of TNFα, MCP-1, IL-1β, and IL-6 in the lung tissue. However, Poldip2 heterozygous deletion reduced cytokine induction. We recently found that heterozygous deletion of Poldip2 *in vivo* also results in impaired cytokine release following cerebral ischemia [17], supporting a role of Poldip2 in modulating the inflammatory response.

In our study, LPS injection led to pronounced leukocyte infiltration into the lung, which was largely prevented by heterozygous deletion of Poldip2. Further characterization of the invading cell populations revealed that deletion of Poldip2 prevented both the early monocyte influx into the alveolar compartment and the delayed neutrophilic response induced by LPS. Previous studies have shown that the interdependence between monocyte and neutrophil trafficking has important implications for the LPS-induced increase in vascular permeability [34]. Monocyte recruitment itself only leads to a modest increase in lung permeability, but greatly amplifies neutrophil recruitment, which has been shown to promote severe lung injury [35,36]. Thus, Poldip2 represents a novel mechanism to regulate leukocyte infiltration, which is central to the pathogenesis of ARDS.

Activated leukocytes adhere firmly to the endothelium via adhesion molecules such as ICAM-1 and VCAM-1, which are members of the immunoglobulin superfamily. ICAM-1 acts as a ligand for the β2 integrins LFA-1 (CD11a/CD18) and Mac-1 (CD11b/CD18) on leukocytes like neutrophils, and VCAM-1 is a receptor for α4β1 integrin (VLA-4) expressed on the surface of activated mononuclear cells (monocytes, T cells, and eosinophils) [37–39]. ICAM-1 and VCAM-1 activation on ECs has been shown to facilitate leukocyte transmigration. Our results show Poldip2 plays a significant role in the regulation of both of these adhesion molecules *in vivo*. Likewise, our *in vitro* investigation showed that depletion of Poldip2 attenuates LPS-induced VCAM-1 induction, potentially through the regulation of mitoROS production. These results are in line with previous evidence indicating Poldip2 participates in ROS regulation [40] and mitochondrial function [41]. However, our report is the first to show that Poldip2 regulates mitochondrial-specific ROS production, although the mechanism by which Poldip2 regulates mitoROS is unknown and warrants further investigation.

Depletion of Poldip2 has been observed to compromise tricarboxylic acid (TCA) cycle activity [41]. It is possible that reduced TCA cycle activity and impaired mitochondrial oxygen consumption could reduce mitoROS production, which could help explain our findings. Likewise, the Poldip2 interacting partner NADPH oxidase 4 (Nox4) is also found within mitochondria [13]. Thus, Poldip2 may also regulate mitoROS production through its interaction with the Nox4 subunit p22phox [40]. The specific downstream consequences of mitoROS regulation by Poldip2 in the

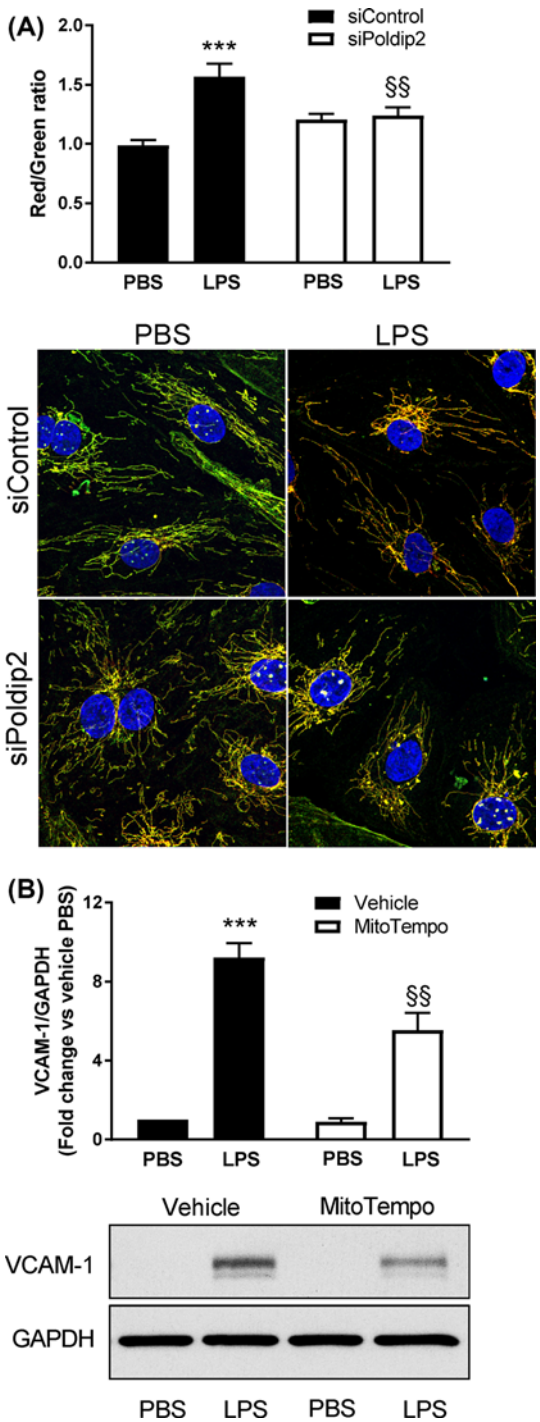

Figure 6. Poldip2 mediates LPS-induced mitoROS production

(**A**) Confluent HPMECs were transfected with siControl or siPoldip2, transduced with mitoTimer and exposed to LPS (100 ng/ml) for 6 h. Quantification of red to green ratio was determined by confocal microscopy. At baseline, mitoTimer fluoresces green. Upon oxidation, mitoTimer shifts to an irreversible red fluorescence. Thus, comparison of red to green fluorescence provides an indirect read-out for mitoROS production. Bars represent means ± S.E.M. of four independent experiments. Two-way ANOVA $^{***}P<0.001$ vs siControl PBS and $^{§§}P<0.01$ vs siControl LPS. (**B**) HPMECs were treated with vehicle or mitoTempo (1 mM) and exposed to LPS (100 ng/ml) for 6 h. VCAM-1 protein expression was measured by Western blotting and densitometry and normalized to GAPDH. Results are presented as fold change with respect to vehicle + PBS. Bars represent means ± S.E.M. of three independent experiments. Two-way ANOVA $^{***}P<0.001$ vs vehicle PBS, $^{§§}P<0.01$ vs vehicle LPS.

Clinical Science (2018) **00** 1–14
https://doi.org/10.1042/CS20180944

regulation of inflammatory signaling are also unknown. VCAM-1 transcription is regulated by AP-1 and NF-κB signaling, both of which are regulated by ROS [42]. Thus, Poldip2-induced mitoROS production may affect these classical VCAM-1 transcription factors. Future research should investigate this potential regulation mechanism.

Future investigation should also focus on further delineating the endothelial role of Poldip2 *in vivo*. In our current model, heterozygous deletion of Poldip2 is protective; however, the cell type or types responsible for the observed benefit are unclear. Pulmonary inflammation and leukocyte infiltration involve various cell types including ECs, epithelial cells, and various immune and blood cells. There is a clear role for ECs in mediating leukocyte adhesion and migration [43], and our *in vitro* data indicate Poldip2 plays a role in this signaling cascade; however, *in vivo* data are lacking. Endothelial-specific Poldip2 deletion *in vivo* could answer this question. Likewise, limited information exists on the role of Poldip2 in leukocyte function, which is a major gap given their importance in mediating the deleterious effects of prolonged inflammation and tissue damage.

The protective response of Poldip2 reduction in the LPS model of ARDS is in agreement with our previous work where monoallelic deletion Poldip2 was found to protect mice from BBB permeability induced by cerebral ischemia [17]. Together, these findings highlight the therapeutic potential of Poldip2 inhibition as a treatment for diseases that elicit severe inflammatory responses, including ARDS, sepsis, and stroke [23,44].

Clinical perspectives

- Acute respiratory distress syndrome (ARDS) is an inflammatory lung condition, for which there exists no targeted treatment strategies, with a current mortality rate ranging from 35 to 46%.
- Monoallelic deletion of polymerase δ-interacting protein 2 (Poldip2) is shown to reduce mortality, inflammation, and lung leukocyte infiltration in a lipopolysaccharide-induced ARDS mouse model.
- Inhibition of Poldip2 may represent an area of therapeutic relevance in the treatment of ARDS.

Competing interests

The authors declare that there are no competing interests associated with the manuscript.

Funding

S.J.F. is supported by N.I.H. 5T32HL007745-24. M.S.H. is supported by AHA 17SDG33410777. K.K.G. is supported by NIH P01 HL095070. R.T.S. is supported by Merit Review VA Award- 5101BX001786-07.

Author contribution

S.J.F., Q.X., and M.S.H. conceived and designed the study. S.J.F. and Q.X. performed the majority of experiments and analyzed data. S.J.F., Q.X., and M.S.H. wrote and edited the manuscript. D.S.K. and E.A.F. helped with cytokine expression assays and tissue sample collection. D.O.-D. performed flow cytometry analysis. A.C.C. helped with mortality analysis and sample collection. B.L. helped with mouse breeding colony maintenance and strategies, provided technical assistance on assays, and helped edit the manuscript. R.T.S. provided guidance and assistance on mouse lung assays reported throughout the manuscript and edited the manuscript. K.K.G. provided expertise, helped with conceptual design, and helped to edit the manuscript. G.Z. provided expertise and helped to edit the manuscript.

Abbreviations

ARDS, acute respiratory distress syndrome; BAL, bronchoalveolar lavage; BBB, blood–brain barrier; CXCL-1, chemokine (C-X-C motif) ligand 1; DMEM, Dulbecco's Modified Eagle's Medium; EC, endothelial cell; HPMECs, human primary pulmonary microvascular endothelial cell; HRP, horseradish peroxidase; ICAM-1, intercellular adhesion molecule 1; IL, interleukin; LPS, lipopolysaccharide; mitoROS, mitochondrial-derived ROS; MCP-1, monocyte chemotactic protein-1; NF-κB, nuclear factor κB; Nox4, NADPH oxidase 4; Poldip2, polymerase δ-interacting protein 2; ROS, reactive oxygen species; RPL, ribosomal protein L13a; siPoldip2, small interfering RNA against Poldip2; siRNA, small interfering RNA; TCA, tricarboxylic acid; TNF-α, tumor necrosis factor-α; VCAM-1, vascular cell adhesion molecule.

References

1 Rubenfeld, G.D., Caldwell, E., Peabody, E., Weaver, J., Martin, D.P., Neff, M. et al. (2005) Incidence and outcomes of acute lung injury. *N. Engl. J. Med.* **353**, 1685–1693, https://doi.org/10.1056/NEJMoa050333

2 Bellani, G., Laffey, J.G., Pham, T., Fan, E., Brochard, L., Esteban, A. et al. (2016) Epidemiology, patterns of care, and mortality for patients with acute respiratory distress syndrome in intensive care units in 50 countries. *JAMA* **315**, 788–800, https://doi.org/10.1001/jama.2016.0291

3 Ragaller, M. and Richter, T. (2010) Acute lung injury and acute respiratory distress syndrome. *J. Emerg. Trauma Shock* **3**, 43–51, https://doi.org/10.4103/0974-2700.58663

4 Fan, E., Brodie, D. and Slutsky, A.S. (2018) Acute respiratory distress syndrome: advances in diagnosis and treatment. *JAMA* **319**, 698–710, https://doi.org/10.1001/jama.2017.21907

5 Herrero, R., Sanchez, G. and Lorente, J.A. (2018) New insights into the mechanisms of pulmonary edema in acute lung injury. *Ann. Transl. Med.* **6**, 32, https://doi.org/10.21037/atm.2017.12.18

6 Grau, G.E., Mili, N., Lou, J.N., Morel, D.R., Ricou, B., Lucas, R. et al. (1996) Phenotypic and functional analysis of pulmonary microvascular endothelial cells from patients with acute respiratory distress syndrome. *Lab. Invest.* **74**, 761–770

7 Park, W.Y., Goodman, R.B., Steinberg, K.P., Ruzinski, J.T., Radella, 2nd, F., Park, D.R. et al. (2001) Cytokine balance in the lungs of patients with acute respiratory distress syndrome. *Am. J. Respir. Crit. Care Med.* **164**, 1896–1903, https://doi.org/10.1164/ajrccm.164.10.2104013

8 Thompson, B.T., Chambers, R.C. and Liu, K.D. (2017) Acute respiratory distress syndrome. *N. Engl. J. Med.* **377**, 1904–1905, https://doi.org/10.1056/NEJMra1608077

9 Thickett, D.R., Armstrong, L., Christie, S.J. and Millar, A.B. (2001) Vascular endothelial growth factor may contribute to increased vascular permeability in acute respiratory distress syndrome. *Am. J. Respir. Crit. Care Med.* **164**, 1601–1605, https://doi.org/10.1164/ajrccm.164.9.2011071

10 Matthay, M.A. and Zemans, R.L. (2011) The acute respiratory distress syndrome: pathogenesis and treatment. *Annu. Rev. Pathol.* **6**, 147–163

11 Azcutia, V., Routledge, M., Williams, M.R., Newton, G., Frazier, W.A., Manica, A. et al. (2013) CD47 plays a critical role in T-cell recruitment by regulation of LFA-1 and VLA-4 integrin adhesive functions. *Mol. Biol. Cell* **24**, 3358–3368

12 Cook-Mills, J.M., Marchese, M.E. and Abdala-Valencia, H. (2011) Vascular cell adhesion molecule-1 expression and signaling during disease: regulation by reactive oxygen species and antioxidants. *Antioxid. Redox Signal.* **15**, 1607–1638

13 Forrester, S.J., Kikuchi, D.S., Hernandes, M.S., Xu, Q. and Griendling, K.K. (2018) Reactive oxygen species in metabolic and inflammatory signaling. *Circ. Res.* **122**, 877–902

14 Hernandes, M.S., Lassegue, B. and Griendling, K.K. (2017) Polymerase delta-interacting protein 2: a multifunctional protein. *J. Cardiovasc. Pharmacol.* **69**, 335–342

15 Chan, J.Y.K., Poon, P.H.Y., Zhang, Y., Ng, C.W.K., Piao, W.Y., Ma, M. et al. (2018) Case Report: exome sequencing reveals recurrent RETSAT mutations and a loss-of-function POLDIP2 mutation in a rare undifferentiated tongue sarcoma. *F1000Res.* **7**, 499

16 Grinchuk, O.V., Motakis, E. and Kuznetsov, V.A. (2010) Complex sense-antisense architecture of TNFAIP1/POLDIP2 on 17q11.2 represents a novel transcriptional structural-functional gene module involved in breast cancer progression. *BMC Genomics* **11**, S9

17 Hernandes, M.S., Lassegue, B., Hilenski, L.L., Adams, J., Gao, N., Kuan, C.Y. et al. (2018) Polymerase delta-interacting protein 2 deficiency protects against blood-brain barrier permeability in the ischemic brain. *J. Neuroinflammation* **15**, 45

18 Sutliff, R.L., Hilenski, L.L., Amanso, A.M., Parastatidis, I., Dikalova, A.E., Hansen, L. et al. (2013) Polymerase delta interacting protein 2 sustains vascular structure and function. *Arterioscler. Thromb. Vasc. Biol.* **33**, 2154–2161

19 Ritz, C. and Spiess, A.N. (2008) qpcR: an R package for sigmoidal model selection in quantitative real-time polymerase chain reaction analysis. *Bioinformatics* **24**, 1549–1551, https://doi.org/10.1093/bioinformatics/btn227

20 Boggy, G.J. and Woolf, P.J. (2010) A mechanistic model of PCR for accurate quantification of quantitative PCR data. *PLoS ONE* **5**, e12355, https://doi.org/10.1371/journal.pone.0012355

21 R: a language and environment for statistical computing [Internet]. *R Foundation for Statistical Computing*, http://www.R-project.org/

22 Laker, R.C., Xu, P., Ryall, K.A., Sujkowski, A., Kenwood, B.M., Chain, K.H. et al. (2014) A novel mitotimer reporter gene for mitochondrial content, structure, stress, and damage in vivo. *J. Biol. Chem.* **289**, 12005–12015, https://doi.org/10.1074/jbc.M113.530527

23 Sheridan, B.C., Dinarello, C.A., Meldrum, D.R., Fullerton, D.A., Selzman, C.H. and McIntyre, Jr, R.C. (1999) Interleukin-11 attenuates pulmonary inflammation and vasomotor dysfunction in endotoxin-induced lung injury. *Am. J. Physiol.* **277**, L861–L867

24 Cirelli, R.A., Carey, L.A., Fisher, J.K., Rosolia, D.L., Elsasser, T.H., Caperna, T.J. et al. (1995) Endotoxin infusion in anesthetized sheep is associated with intrapulmonary sequestration of leukocytes that immunohistochemically express tumor necrosis factor-alpha. *J. Leukoc. Biol.* **57**, 820–826, https://doi.org/10.1002/jlb.57.6.820

25 Muller, A.M., Cronen, C., Muller, K.M. and Kirkpatrick, C.J. (2002) Heterogeneous expression of cell adhesion molecules by endothelial cells in ARDS. *J. Pathol.* **198**, 270–275, https://doi.org/10.1002/path.1186

26 Cheng, X., Kanki, T., Fukuoh, A., Ohgaki, K., Takeya, R., Aoki, Y. et al. (2005) PDIP38 associates with proteins constituting the mitochondrial DNA nucleoid. *J. Biochem.* **138**, 673–678, https://doi.org/10.1093/jb/mvi169

27 Arakaki, N., Nishihama, T., Kohda, A., Owaki, H., Kuramoto, Y., Abe, R. et al. (2006) Regulation of mitochondrial morphology and cell survival by Mitogenin I and mitochondrial single-stranded DNA binding protein. *Biochim. Biophys. Acta* **1760**, 1364–1372, https://doi.org/10.1016/j.bbagen.2006.05.012

28 Lyle, A.N., Deshpande, N.N., Taniyama, Y., Seidel-Rogol, B., Pounkova, L., Du, P. et al. (2009) Poldip2, a novel regulator of Nox4 and cytoskeletal integrity in vascular smooth muscle cells. *Circ. Res.* **105**, 249–259, https://doi.org/10.1161/CIRCRESAHA.109.193722

29 Murphy, M.P. and Smith, R.A.J. (2007) Targeting antioxidants to mitochondria by conjugation to lipophilic cations. *Annu. Rev. Pharmacol. Toxicol.* **47**, 629–656, https://doi.org/10.1146/annurev.pharmtox.47.120505.105110

30 Bastarache, J.A. and Blackwell, T.S. (2009) Development of animal models for the acute respiratory distress syndrome. *Dis. Model Mech.* **2**, 218–223, https://doi.org/10.1242/dmm.001677
31 Gandhirajan, R.K., Meng, S., Chandramoorthy, H.C., Mallilankaraman, K., Mancarella, S., Gao, H. et al. (2013) Blockade of NOX2 and STIM1 signaling limits lipopolysaccharide-induced vascular inflammation. *J. Clin. Invest.* **123**, 887–902
32 Springer, T.A. (1994) Traffic signals for lymphocyte recirculation and leukocyte emigration: the multistep paradigm. *Cell* **76**, 301–314, https://doi.org/10.1016/0092-8674(94)90337-9
33 Bobrowski, W.F., McDuffie, J.E., Sobocinski, G., Chupka, J., Olle, E., Bowman, A. et al. (2005) Comparative methods for multiplex analysis of cytokine protein expression in plasma of lipopolysaccharide-treated mice. *Cytokine* **32**, 194–198, https://doi.org/10.1016/j.cyto.2005.09.007
34 Maus, U., von Grote, K., Kuziel, W.A., Mack, M., Miller, E.J., Cihak, J. et al. (2002) The role of CC chemokine receptor 2 in alveolar monocyte and neutrophil immigration in intact mice. *Am. J. Respir. Crit. Care Med.* **166**, 268–273, https://doi.org/10.1164/rccm.2112012
35 Sibille, Y. and Reynolds, H.Y. (1990) Macrophages and polymorphonuclear neutrophils in lung defense and injury. *Am. Rev. Respir. Dis.* **141**, 471–501, https://doi.org/10.1164/ajrccm/141.2.471
36 Wagner, J.G. and Roth, R.A. (1999) Neutrophil migration during endotoxemia. *J. Leukoc. Biol.* **66**, 10–24, https://doi.org/10.1002/jlb.66.1.10
37 Smith, C.W., Marlin, S.D., Rothlein, R., Toman, C. and Anderson, D.C. (1989) Cooperative interactions of LFA-1 and Mac-1 with intercellular adhesion molecule-1 in facilitating adherence and transendothelial migration of human neutrophils in vitro. *J. Clin. Invest.* **83**, 2008–2017, https://doi.org/10.1172/JCI114111
38 Elices, M.J., Osborn, L., Takada, Y., Crouse, C., Luhowskyj, S., Hemler, M.E. et al. (1990) VCAM-1 on activated endothelium interacts with the leukocyte integrin VLA-4 at a site distinct from the VLA-4/fibronectin binding site. *Cell* **60**, 577–584, https://doi.org/10.1016/0092-8674(90)90661-W
39 Staunton, D.E., Marlin, S.D., Stratowa, C., Dustin, M.L. and Springer, T.A. (1988) Primary structure of ICAM-1 demonstrates interaction between members of the immunoglobulin and integrin supergene families. *Cell* **52**, 925–933, https://doi.org/10.1016/0092-8674(88)90434-5
40 Lyle, A.N., Deshpande, N.N., Taniyama, Y., Seidel-Rogol, B., Pounkova, L., Du, P. et al. (2009) Poldip2, a novel regulator of Nox4 and cytoskeletal integrity in vascular smooth muscle cells. *Circ. Res.* **105**, 249–259, https://doi.org/10.1161/CIRCRESAHA.109.193722
41 Paredes, F., Sheldon, K., Lassègue, B., Williams, H.C., Faidley, E.A., Benavides, G.A. et al. (2018) Poldip2 is an oxygen-sensitive protein that controls PDH and αKGDH lipoylation and activation to support metabolic adaptation in hypoxia and cancer. *Proc. Natl. Acad. Sci. U.S.A.*, https://doi.org/10.1073/pnas.1720693115
42 Manea, S-A, Constantin, A., Manda, G., Sasson, S. and Manea, A. (2015) Regulation of Nox enzymes expression in vascular pathophysiology: focusing on transcription factors and epigenetic mechanisms. *Redox Biol.* **5**, 358–366, https://doi.org/10.1016/j.redox.2015.06.012
43 Ley, K., Laudanna, C., Cybulsky, M.I. and Nourshargh, S. (2007) Getting to the site of inflammation: the leukocyte adhesion cascade updated. *Nat. Rev. Immunol.* **7**, 678, https://doi.org/10.1038/nri2156
44 Huang, J., Upadhyay, U.M. and Tamargo, R.J. (2006) Inflammation in stroke and focal cerebral ischemia. *Surg. Neurol.* **66**, 232–245, https://doi.org/10.1016/j.surneu.2005.12.028